

# Recent results on GDR pre-equilibrium $\gamma$ -ray emission

Massimo Papa

*Istituto Nazionale di Fisica Nucleare - Sezione di Catania - Via S.Sofia 64 I-95123.*

*Catania Italy*

**Abstract.** Recent experimental results on GDR  $\gamma$ -ray pre-equilibrium emission induced on the  $^{40}\text{Ca}+^{48}\text{Ca}$  system at 10 and 25 MeV/nucleon have been illustrated. The interpretation of the obtained results in the framework of the CoMD-II approach to the N-Body dynamics allow an interpretation of the observed phenomenon as a measure of the surviving of collective dipolar motion excited on the hot intermediate compound and as a finger print of the isospin equilibration process.

**Keywords:** Pre-equilibrium, GDR, Isospin, N-body approach.

**PACS:** 24.10-i, 24.60.-k, 24.30.Cz, 21.60.-n.

## I. INTRODUCTION

Pre-equilibrium effects have a quite high relevance in nuclear dynamics. A part from the peculiarity of reaction mechanism itself, they allow having access to the first moments of the interaction between the colliding partners and therefore can be able in principle to probe states of nuclear matter very far from the ground states properties.

On the other hand pre-equilibrium effects are well localized in time and at longer time the studied process are dominated by statistical decays of the produced hot sources. These conditions on one hand ask for the definition of observables which should have a weak dependence from the secondary decay process, and on the other make necessary the usage of self-consistent fully N-body approach to describe the dynamics of the phenomenon up to the typical equilibration times of the studied processes.

In the present contribution we will focus on the GDR pre-equilibrium phenomenon [1-28].

Pre-equilibrium effects were evidenced at low energy in fusion reactions [6,11,23] and binary processes for different systems [9,10,13,14,21,22,24].

We will try to illustrate, starting from recent experimental results obtained for the  $^{40}\text{Ca}+^{48}\text{Ca}$  and  $^{40}\text{Ca}+^{46}\text{Ti}$  systems, some examples of the problems above outlined.

In particular in Sec.II we will briefly discuss the measurement on these systems at 25 MeV/nucleon.

In this measurement GDR dynamical pre-equilibrium emission was evidenced in incomplete fusion and binary dissipative reactions by using  $\gamma$ -ray-particle coincidence method.

In Sec.II section more emphasis is placed on the fluctuating dynamics. In the same experiment in fact also a suppression of the GDR yield was observed at higher  $\gamma$  energy for incomplete fusion processes around 15 MeV. The analysis performed in the framework of the statistical model shows the survival of the GDR mode up to excitation energy of about 5 MeV/nucleon of the hot compound having mass around 60. For a given system this limiting energy, as proposed in ref. [27, 28], is linked with the excitation energy to which a liquid-gas phase transition should begin. By using calculations based on the Constrained Molecular Dynamical model [29] it is possible to estimate the  $\gamma$ -ray yield related to both the statistical emission and the dynamical one. In the frame-work of this full N-body approach the suppression of the GDR mode it is strongly related to the non-equilibrium effects of the fluctuating dynamics of the GDR mode. By performing calculations at different incident energies we will also show that the ratio between the dynamical yield and the statistical one (or the degree of coherence) is a quite sensitive observable strongly linked with the degree of collectivity of the dipolar mode.

In Sec. III we will illustrate the very last experimental results collected on the pre-equilibrium GDR emission for the same colliding nuclei at 10 MeV/nucleon in coincidence with binary dissipative events. In this case we will describe with some more details the study performed to evidence the effect of the average dynamics.

The investigation performed on these systems allows to clearly linking the measured pre-equilibrium  $\gamma$ -ray extra-yield for the  $^{40}\text{Ca}+^{48}\text{Ca}$  collision with the isospin equilibration process on the final fragments. In particular it will be shown that, at the involved energy, the intensity of the pre-equilibrium emission reveals a quasi-resonant mechanisms for the charge/mass equilibration process. The performed study put also in evidence that average time derivative of the total dipole  $\overline{V}$  is a global variable gives a measure of the “isospin” flow in the studied system. This global variable is invariant with respect to statistical emission processes which we can suppose to take place after an equilibration time  $t_{\text{eq}}$

## II. $^{40}\text{Ca}+^{48}\text{Ca}$ , $^{46}\text{Ti}$ 25 MEV/NUCLEON

As quoted in the previous section in several experiments around 8-10 MeV/nucleon it was pointed out that the  $\gamma$ -ray yield is increased with respect to statistical calculations in the region around 10 MeV, for systems with mass lower than 150 and having a pronounced difference in the charge/mass ratio between projectile and target.

This enhancement was ascribed, according to various theoretical arguments, to pre-equilibrium effects (see for example [6,14,30,31,37]). In some of these works (see for example [14,37]) an estimation of the pre-equilibrium yield in absolute units has also been given.

The prediction was obtained in the semi classical approximation, by applying the Larmor formula to the dipole, obtaining a satisfactory agreement with the data. A comparison with the statistical model, based on the local time equilibrium hypothesis, was also performed [14].

More recently these kinds of studies have been performed on the systems  $^{40}\text{Ca}+^{48}\text{Ca}$  and  $^{40}\text{Ca}+^{46}\text{Ti}$  at 25 MeV/nucleon [20]. The second system has been taken as a reference system: in fact for the system  $^{40}\text{Ca}+^{46}\text{Ti}$  this pre-equilibrium effect is negligible because of the very similar charge/mass ratio between projectile and target. For central collisions the  $^{40}\text{Ca}+^{48}\text{Ca}$  system shows an extra-yield of about 50% at 10 Me with an intensity at the maximum of about  $2 \times 10^{-4} \text{ MeV}^{-1}$  [21].

So far the dynamical studies on this subject have been performed using a semi-classical mean field theory (see also ref. [36]). However, especially in the Fermi energy domain, the role played by the fluctuations around the mean values should be investigated in a consistent way using a dynamical approach. In fact for the  $\gamma$ -ray emission at these energy or higher, many of the investigated systems (see [28]) shows anomalies in the region in which the GDR statistical emission is prominent.

In Figure 1, (left part) we show the experimental results obtained for the systems under study. The lines in the panels represent the fit with CASCADE calculations applied to a hot compound of mass  $A \approx 60$  excited to estimated excitation energy of about 6 MeV/nucleon. To reproduce the data it is necessary to impose an excitation energy cut-off for the GDR emission of about 5.4 MeV/nucleon for the  $^{40}\text{Ca}+^{48}\text{Ca}$  system and about 4.7 MeV/nucleon for the  $^{40}\text{Ca}+^{46}\text{Ti}$ .

In this section, for the investigated systems, we will try to illustrate the study performed on the interplay between pre-equilibrium effect on the statistical emission and on the dynamical or the coherent one. To this aim we will use the Constrained Molecular Dynamics model (CoMD) [29]. The model takes into account the effect of the Fermionic nature of the nuclear many-body system by constraining the phase space to fulfil at each time step the Pauli principle.

### General framework

To present the main line of investigation suggested by this dynamical approach, in Figure 1 (right panel) we show, as an example, the time derivative of the total dipole, along the beam direction,  $\dot{V}_z$  as function of time.

In the figure we show three typical events representing the system  $^{40}\text{Ca}+^{48}\text{Ca}$  at 25 MeV/nucleon in a central collision. For the present study we have generated all the events by initializing the colliding system with identical

macroscopic initial conditions (same impact parameter, same total spin, and same incident energy). The time derivative of these quantities is directly linked with the  $\gamma$ -ray emitted power. The three curves, plotted with different symbols, show very similar behaviour in the first 100 fm/c.

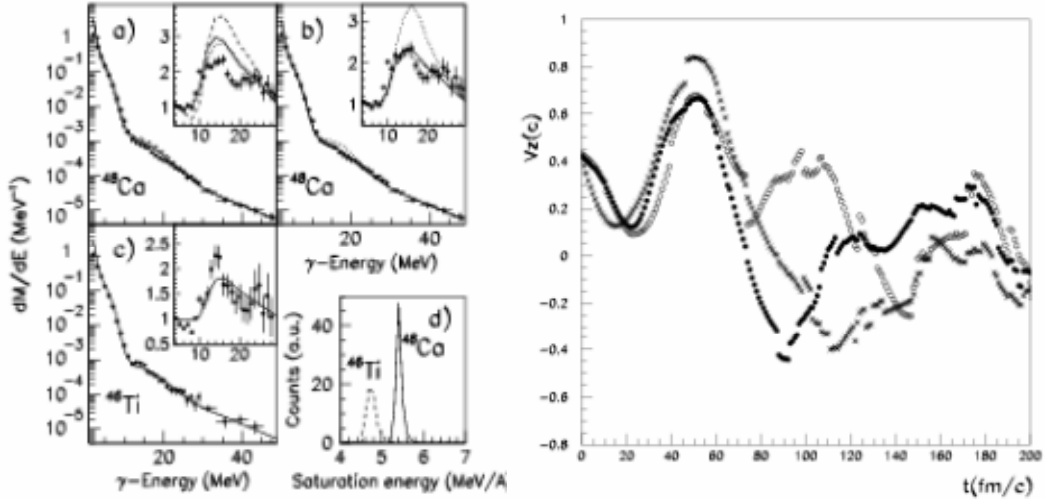


**FIGURE 1.** Left panels: experimental  $\gamma$ -ray spectra compared with CASCADE calculations [20]. Right panel: time derivative of the total dipole, along the beam direction,  $V_z$  for different CoMD events calculated for the  $^{40}\text{Ca}+^{48}\text{Ca}$  collision at 25 MeV/nucleon [21].

This similarity determines an ensemble average different from zero. The average shows quasi-periodicity and gives rise to the coherent contribution to the collective neutron-proton motion. After some time the three signals lose their phase relations, even though they are always characterized by an oscillating behavior. This on the one hand will damp the coherent mode, but on the other hand will give rise to the so-called fluctuating (with respect to the ensemble average) or incoherent collective motion. This kind of behaviour is able to mimic the statistical emission of a hot compound system.

Finally all the signals at different times show discontinuities produced by the nucleon-nucleon scattering process. This microscopic incoherent motion (or non collective) will contribute to the GDR damping. It will also determine the high energy spectral properties of the emitted radiation or the so-called bremsstrahlung contribution.

All these contributions and their interplay are interesting for several reasons. For example:

-i) the strength connected to the fluctuating or incoherent dipolar collective excitations should correspond, for a fully equilibrated system, to the strength predicted by the statistical Compound Nucleus theory included in the statistical code CASCADE [32].

-ii) both the dynamical stage and the onset of fluctuations on the collective coordinate can be affected by the formation of fragments during the multi-fragmentation of a hot source induced by the heavy ion collision. This effect needs a fully dynamical study of the many-body problem including the reaction dynamics. In general it cannot be investigated by means of statistical models or hybrid models.

In the following we will try to discuss these different aspects by comparing the model calculations with experimental results for central collisions [20].

### Coherent emission in the $^{40}\text{Ca}+^{48}\text{Ca}$ system

In this section we briefly recall the main results obtained from dynamical calculations concerning the prediction on the coherent contribution. More details can be found [20].

For the studied systems several hundreds of events have been generated. A selection of the events leading to incomplete fusion process has been performed.

On this restricted sample of events we have computed the ensemble average for the time derivative of the total dipole :

$$\bar{\vec{V}} = \sum_{i=1,Z} \frac{d\bar{r}_i}{dt} \quad (1)$$

The bar in the previous expression indicates the ensemble average. The  $\gamma$ -ray emission probability for energy unit was calculated by means of the Fourier transform of the time derivative of the k components X and Z of according to the following relation:

$$\frac{dP}{dE} = \frac{4e^2}{6\pi\hbar cE} \left| \frac{d\bar{V}_k}{dt}(E) \right|^2 ; \quad \frac{d\bar{V}_k}{dt}(E) = \int_0^{\infty} \frac{d\bar{V}_k}{dt}(t) e^{i\frac{Et}{\hbar c}} dt \quad (2)$$

dP/dE has to be interpreted as the average number of  $\gamma$ -rays emitted for energy unit.

The total strength shows a dependence on the impact parameter. The maximum is obtained for the impact parameters in the range  $b=2-5$  fm. The intensity at the maximum for  $b$  around 4 fm, which represents the centroid of the selected  $b$ -window is about  $2 \times 10^{-4} \text{ MeV}^{-1}$ . This value is in good agreement with the experimental one at 11 MeV [21].

### The incoherent contribution

In this section we want to describe the procedure used to evaluate from CoMD calculations the statistical contribution to the GDR  $\gamma$ -ray emission. This subject, if treated with N-body approach, can reveal considerable difficulties. One of these is the time necessary to describe the incoherent emission. The statistical emission can in fact go on up to several thousands of fm/c. Another difficulty is the definition of temperature.

This definition is encountered when a necessary comparison of our model description is done with statistical model prediction over long times. Determining a time interval after which the thermal equilibrium (with respect to the GDR mode) is reached by our system solves the first problem. To obtain this, using our Fourier analysis, it will be enough to follow the dynamical evolution up to 1000 fm/c. We have solved the second problem by comparing our predictions with a simple and well-known dynamical model based on the Langevin equation in which the temperature characterizes the behavior of the stochastic force.

In the framework of the Langevin approach the asymptotic prediction concerning the yield of the GDR  $\gamma$ -ray emission corresponds to the well known expression which characterizes the CASCADE calculation [32].

### Incoherent emission in the $^{40}\text{Ca}+^{48}\text{Ca}$ system at 25 MeV/nucleon

For the same set of events for which we have deduced the average properties of the generic dipolar component, we can compute the power connected to the fluctuating or incoherent one. In particular the second time derivative of the incoherent dipolar signals is given by the following relation:

$$\frac{dV_{k,f}^i}{dt} = \frac{dV_k^i}{dt} - \frac{d\bar{V}_k}{dt} \quad (2)$$

With a Fourier analysis it is possible to calculate the number of  $\gamma$ -rays per energy unit emitted through the incoherent mechanism by applying the relations (1) to the fluctuating mode evaluated through the above equation. To this aim the dynamics has been followed up to 1000 fm/c.

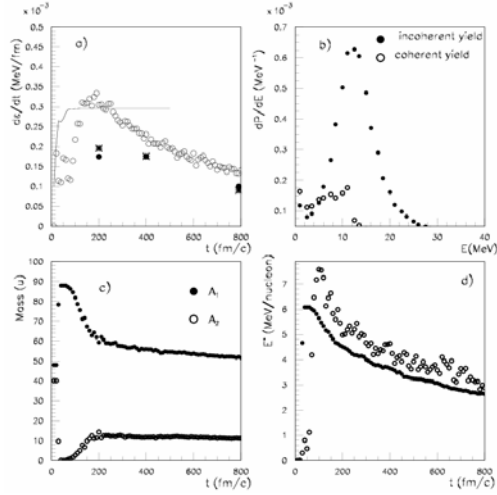


**FIGURE 2.** For  $E_{\text{lab}}=25$  MeV/nucleon and  $b=0$  fm; a) emitted power through the incoherent mechanism related to the Z component, as function of time (empty circles) evaluated with CoMD calculations. The full circles represent the prediction of the CASCADE calculations for the collective emitted power. The star symbol represents the same quantity as predicted by CoMD calculations. The line represents the emitted power as produced by Langevin calculations applied to the total system; b) related  $\gamma$ -ray emission spectra for the incoherent (full circles) mechanism and for the coherent mechanisms (empty circles); c) average mass of the two largest fragments; d) related average excitation energy per nucleon (from ref.[21]).

As an example results of the described calculations are shown in Figure 2 for the  $^{40}\text{Ca}+^{48}\text{Ca}$  system at 25 MeV/nucleon and for central collision ( $b=0$  fm).

In the upper panel a) the power emitted as function of time (collective plus bremsstrahlung contributions) related to the Z component is shown with empty circles, the stars and the full line represent predictions according to the standard statistical model calculations or Langevin calculations as we will explain in the following.

The full circles represent the collective contribution as obtained by CoMD calculations. In panel b) we show the average multiplicity distribution  $dP/dE$  connected to the incoherent collective process along the Z axis (full circles) and those connected to the coherent process (empty circles).

Finally, in panel c) the average masses corresponding to the two largest fragments and, in panel d), the related excitation energies as a function of time are shown. The average multiplicity distribution shown in Figure 2b) is peaked around 15 MeV. This indicates that the evaluated incoherent contribution has essentially a collective character. However, the incoherent yield also shows, in a semi-logarithmic plot, a typical high energy tail related to the bremsstrahlung contribution (see also Figure 9 of ref.[21]).

The width of the energy distribution shown in panel b) is about 9 MeV. It is about 1.7 times the "ground state" one evaluated with the same approach.

It has to be noted, however, that the multiplicity distribution shown in Figure 2b) is the global result of a hot source which rapidly changes mass and excitation energy (see panel c) and d)).

In particular, in a short time the residues reach an excitation energy of about 5 MeV/nucleon and a mass of about 60 units. At this time the incoherent collective power is at the maximum. Therefore the obtained results are substantially in agreement with the analysis performed in ref.[20]. The changes in the following 600 fm/c are smaller.

Looking at the system behavior during a short time interval, clear pre-equilibrium effects can be seen from Figure 2a). In particular in the first 200 fm/c the power emitted via the incoherent mechanism increases up to a maximum value corresponding to the formation (on average) of the two main fragments. During this stage the collision rate increases practically with the same profile. The curve represents a prediction based on the Langevin approach in which the damping parameter  $\Gamma$  and the resonant energy  $E_0$  are computed from the  $\gamma$ -ray spectra obtained with CoMD calculations. The mass A and the charge are those of the total system. The temperature has been computed from the usual relation for Fermionic systems  $E^*=aT^2$  with  $a=A/12$  (the choice for the value of this parameter is discussed in the next section).

After a very short transient connected to the  $\Gamma$  parameter, we observe that the Langevin calculations (line in Figure 2a)), give a stationary value corresponding to the one predicted by statistical calculation (see Eq.(A.9) in ref.[21]).

This comparison shows that in this first stage the pre-equilibrium effect connected to the incoherent process is dominated by the finite time in which the collision rate (acting in this case as a noise able to excite the dipolar mode) increases. This time is larger than what the Langevin approach predicts, since the system at this stage is not in thermal equilibrium with respect to the GDR mode. We note also that in the first 50-70 fm/c the emitted power evaluated with our calculations displays sharp peaks which cannot be produced with the Langevin approach. These peaks originate from Coulomb and compression effects arising when the two nuclei start to overlap. Moreover, on average, a fragment starts to separate quickly from the total system (see Figure 2c), and after 200 fm/c it is completely formed.

### *Comparison with the Langevin approach*

To make a detailed comparison with statistical model calculations concerning the GDR mode, we have to disentangle between collective and non-collective or bremsstrahlung motion related to the total dipole. To make this comparison we used the following procedure: at different time intervals the spectrum of the emitted radiation has been evaluated through a Fourier analysis (see the Appendix B of ref.[21]). The obtained spectra have been fitted with a function  $F(E)$  reflecting the standard statistical model formula plus an essentially exponential term able to reproduce the long tail related to the non-collective contribution. From this procedure we have obtained the so-called temperature  $T$ , the GDR centroid and the damping width parameter. These parameters describe the statistical collective mode through the first term  $F_R$  of the function  $F(E)$ . This procedure has been applied at different times and the extracted values of the  $T$  parameter have been correlated, by means of the well known relation  $E^*=A/gT^2$ , to the calculated excitation energy of the hot source obtained from the CoMD calculations (see Figure 2d) and Figure 2c)). The emitted power related to  $F_R(E)$  represents the collective energy-weighted yield due to the motion along the  $Z$  direction produced by the dynamical model. It is shown with full circles in Figure 2a) at different times.

We note that in the equilibrium statistical model the yield is proportional to the following parameter;

$$\beta = \frac{4e^2 NZ\Gamma}{3m_0 A\pi\pi(\hbar c)^2} .$$

It is determined by the mass, charge and damping width of the emitting source. Therefore,

using the average value of the above expression as evaluated with CoMD calculations, instead of the  $\beta$  value as extracted through the fit procedure, we can obtain also an estimation of the predicted strength according to the statistical calculations in the local time equilibrium hypothesis. The results are shown in Figure 2a) as stars, for different times. From the calculations described it results that at  $E_{lab}= 25$  MeV/nucleon and for times greater than 200 fm/c, the CoMD predictions are in agreement with the statistical model (in the local time equilibrium hypothesis). This agreement is strongly supported by the fact that the  $g$  parameter used in the above-mentioned fit procedure assumes the value 12 at different impact parameters and at different times, within 10%. The stability of this parameter and its value, which is quite reasonable, means also that CoMD calculations at relatively low energy and for times longer than the fragment formation one, produces fluctuations on the collective mode which have a reasonable size.

## **Coherent and Incoherent contribution**

For central collisions ( $b=0$  fm) we have performed calculations also at 35 and 50 MeV/nucleon. At these energies the hot sources disassemble producing, on average, a third cluster. The size of the largest fragment decreases by increasing energy. The fragment formation process takes a shorter time, about 150 fm/c and 100 fm/c at 35 and 50 MeV/nucleon respectively.

In Figure 3a),3d) and for the 50 MeV/nucleon case we plot the quantities as shown in Figure 2a),2d).

As displayed in Figure 3d), the largest fragment reaches an average excitation energy of 5 MeV/nucleon within 100 fm/c. In panel a) of the same Figure we show the emitted  $\gamma$ -ray power as a function of time produced by the incoherent mechanism. The same criteria as for the 25 MeV/nucleon case have been used to estimate the collective yields, as given by the dynamical model, and the ones expected from the statistical model.

At variance with the lower energy case, we note that around the time of the fragments formation, the predictions of the statistical model calculations overestimate the incoherent collective power emitted as predicted by our dynamical model. This effect is quite evident at 50 MeV/nucleon. This suggests that by increasing the energy given to the system the fluctuations in the collective mode are no longer in agreement with the predictions given by the Langevin approach or the standard statistical theory. These deviations are more pronounced in the first stage of the

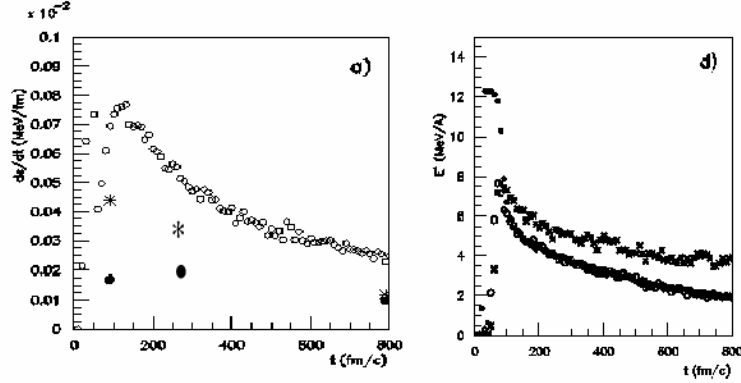


FIGURE 3. Panel a) and d) displays the same quantities like the ones of Figure 2. but for the  $^{40}\text{Ca}+^{48}\text{Ca}$  system at 35 MeV/nucleon.

interaction and they can show up also after the fast fragment formation process when CASCADE calculations are usually applied.

This instability effects can be investigated, as it is usually done, by looking at many body quantities like the fragments, their energy and mass distributions. The same calculations produce (see ref.[21]) the typical conditions for a phase transition with a power law for the mass distributions and bending of the Campi-plot are clearly evident.

For a system undergoing a multi-fragmentation process, this analysis seems therefore to suggest a growth of fluctuations on the dipolar mode and a decreasing collective contribution with respect to the standard statistical model. This means that, at a macroscopic level, the equation of motion of the dipole deviates from the simple prescription of a Langevin approach described in the Appendix A. This deviation seems not due to well-known effects like those that can be taken into account using a local time equilibrium hypothesis as previously discussed.

On the contrary, this deviation seems to arise from a more complex form of the effective Hamiltonian describing the collective mode during a multi-fragmentation process or it can be simply related to the inapplicability of the temperature concept for the collective motion.

#### *Degree of dipolar collectivity in central collision as function of energy*

To make more quantitative the study performed, in this section we estimated a degree of collectivity for the incoherent motion in central collisions .

For this purpose, using the fit procedure described in the previous section, we can estimate the total  $\gamma$  energy  $\varepsilon_{Es,c}(t_1,t_2)$  emitted in the generic time interval  $t_2-t_1$  with energy  $E \leq E_s$  through the collective mode ( $E_s$  was fixed at 35 MeV) and the one including also the bremsstrahlung process  $\varepsilon_{Es}(t_1,t_2)$ .

Starting from these quantities we then define a degree of collectivity at different time intervals as:

$$\varphi_c(0,t) \equiv \frac{\varepsilon_{Es,c}(0,t)}{\varepsilon_{Es}(0,t)} , \quad \varphi_c(t,tm) \equiv \frac{\varepsilon_{Es,c}(t,tm)}{\varepsilon_{Es}(t,m)} \quad (3)$$

$t$  has been chosen as the time of the hot sources fragmentation  $t_f$ . Its value is about 180 fm/c 135 fm/c and 90fm/c at 25 MeV/nucleon, 35 MeV/nucleon and 50 MeV/nucleon respectively;  $tm$  is the maximum time of the calculation and was fixed at 1000 fm/c. The results of these calculations are shown in Table 1.

By comparing the results of the second and third column, it becomes evident that the degree of collectivity is not uniformly distributed in time. In particular  $\varphi_c(t_f,tm)$  slowly decreases with the energy. Fast changes and a much lower value of the collectivity are instead observed during and before the fragment formation as one can see from the behavior of  $\varphi_c(0,t_f)$  . This time region is the same where the strongest deviations from the standard statistical model have been discussed in the previous section.

It is worthwhile noting that remarkable changes are between 25 and 35 MeV/nucleon when the multi-fragmentation process sets in. This suggests a strong correlation of the phenomenon with the disassembly of the system and with the increasing of the bremsstrahlung contribution.

From our calculations, it results that the  $NZ/A$  value necessary to get the agreement with the statistical model calculations is lower than the calculated value obtained through the dynamical approach by looking at the charge and mass of the hot source. This clearly gives strong support to the existence of pre-equilibrium effects of the incoherent or statistical emission mechanism produced by the separation of different phases in the system. A possible explanation is that during the fragment formation process only a reduced number of nucleons are able to follow a collective mode because of the redistribution of the nucleons into different fragments.

**TABLE 1.** Time dependence of the degree of collectivity and degree of coherence at different incident energies

$E_{\text{lab}}$ MeV/nucleon	$\varphi_c(\text{tf},\text{tm})$	$\varphi_c(\mathbf{0},\text{tf})$	$\varphi_{\text{ch}}(\mathbf{0},\text{tm})$	$\varphi_{\text{ch}}(\text{tf},\text{tm})$	$\varphi_c'(\text{tf},\text{tm})$	$\varphi_c'(\mathbf{0},\text{tf})$	$\varphi_{\text{ch}}'(\mathbf{0},\text{tm})$
25	0.89	0.78	0.095	$\sim 0$	1	1	1
35	0.86	0.62	0.064	$\sim 0$	0.96	0.80	0.67
50	0.83	0.58	0.059	$\sim 0$	0.93	0.74	0.62

We conclude this section by observing that the large changes of the degree of collectivity, being concentrated in short time, involve only a small fraction of the total yield. This obviously can make, in some cases, the experimental investigation rather ambiguous.

#### *Degree of Coherence*

We can now define a degree of coherence  $\varphi_{\text{ch}}(\mathbf{0},\text{tm})$  for the collective motion by performing the ratio between the total energy emitted via the coherent mechanism and the one emitted by the incoherent one according to the following relation:

$$\varphi_{\text{ch}}(t, \text{tm}) \equiv \frac{\varepsilon_{Es,\text{ch}}(t, \text{tm})}{\varepsilon_{Es}(t, m)} \quad (4)$$

where the quantity  $\varepsilon_{Es,\text{ch}}(\mathbf{0},\text{tm})$  is the analogue of  $\varepsilon_{Es,c}(\mathbf{0},\text{tm})$  but it is relative to the emitted power connected to the coherent process.  $Es$  in this case has been set equal to 20 MeV.

In this parameter, which is clearly related to memory effects of the GDR dynamics, we can expect that some model dependence concerning the evaluation of the  $\gamma$ -ray strength are removed by definition, because of the ratio between the emitted powers related to the two mechanisms.

The results for  $\varphi_{\text{ch}}$  are shown in Table 1 in the fourth column. It is remarkable that the behaviour of the degree of coherence resembles the behavior of the degree of collectivity  $\varphi_c(\mathbf{0},\text{tf})$  of the process which has been defined in a time interval around the fragment formation process.

In particular large changes are observed between 25 and 35 MeV/nucleon when the instability leading to the fragment formation sets in. This similar behavior is better seen by looking at the columns 6, 7 and 8 of Table I in which the degree of collectivity and the degree of coherence have been normalized to the 25 MeV/nucleon case. They have been indicated with the corresponding primed symbols.

From this analysis it seems that the degree of collectivity of the incoherent contribution in the first  $\sim 150$  fm/c and the degree of coherence of the mode are linked. Moreover the relative changes of the degree of coherence appear to be also more sensitive to the variation of the bombarding energy and to the related reaction mechanism. Contrary to the degree of collectivity, this sensitivity is maintained also asymptotically in time (see also column 6 in Table 1.).

We conclude this section by observing that, from an experimental point of view, the study of the coherent contribution can be performed like in the last experiment [21,38] through a direct comparison between very similar systems having only large differences in the charge/mass symmetry of the two partners (see next section).

The studies performed in this section suggest that the measurement of the degree of coherence as function of the incident energy can give information on the collective behaviour of the nuclear matter in an independent way from

equilibrium statistical model calculations. In particular the extracted information is linked, in a quite sensitive way, to the properties of the hot short living total intermediate system.

### III. $^{40}\text{Ca}+^{48}\text{Ca}, ^{46}\text{Ti}$ 10 MEV/NUCLEON

In this section we will illustrate the last results obtained for the coherent GDR emission in binary dissipative process induced on the system  $^{40}\text{Ca}+^{48}\text{Ca}, ^{46}\text{Ti}$  a 10 MeV. After a short illustration of the main criteria adopted for the analysis and the comparison with calculation we will give an estimation of the degree of coherence a we will try to show the existence of a clear link can be established between the isospin equilibration process and the intensity of the dynamical  $\gamma$ -ray yield [38].

To characterize the degree of charge/mass asymmetry of a binary system, we will use in the calculations the following parameter [13,14]

$$R_{NZ} = \frac{1}{2} \frac{A_1 A_2}{A_1 + A_2} \left( \frac{N_1 - Z_1}{A_1} - \frac{N_2 - Z_2}{A_2} \right) \quad (5)$$

$N$ ,  $Z$ , and  $A$  are the neutron, proton and mass numbers of the two partners 1 and 2 respectively.

$R_{NZ}$  determines the initial amplitude of the dipolar signal for a binary system due to the partition of the total mass and charge between the two partners. This is clearly related to the so called isospin asymmetry differences of the two nuclei. For the two investigated the initial values of these parameters are the following:  $R_{NZ} (^{40}\text{Ca}+^{48}\text{Ca})=1.81$  and  $R_{NZ} (^{40}\text{Ca}+^{48}\text{Ti})=0.46$ .

### The experiment

As for the data collected at 25 MeV/nucleon, the experiment was performed at the Superconducting Cyclotron of the Laboratori Nazionali del Sud (LNS), Catania (Italy). A 9.5 MeV/nucleon and 10 MeV/nucleon beam of  $^{40}\text{Ca}$  was used impinging on 3 mg/cm<sup>2</sup> and 2 mg/cm<sup>2</sup> thick targets of  $^{48}\text{Ca}, ^{46}\text{Ti}$  respectively.

We used the 63 BaF<sub>2</sub> crystals of the multi-detector TRASMA.. The BaF<sub>2</sub> were placed in a cluster configuration (7 crystals for each cluster) around 45<sup>0</sup>, 90<sup>0</sup> and 135<sup>0</sup>.

We performed the neutron subtraction using both time of flight and pulse shape information from the BaF<sub>2</sub> detectors. The monitoring of the phototube gains was performed by repeating the calibration procedure several times during the experiment.

Charged fragments in coincidence with  $\gamma$ -rays were detected by 120 units of monolithic silicon telescopes. More details on the experimental apparatus can be found in ref.[20,34-36]. With our particle detectors we can measure the charge  $Z$  of the detected particles. In order to get the velocity and kinematical information, to better characterize the studied processes, we assume the fragment mass  $A$  of the detected particle equal to the mass of the stable isotope having the charge  $Z$ .

### Results

#### *Selection of binary reactions*

In this section we present the results obtained for the coherent pre-equilibrium  $\gamma$ -ray emission produced in binary processes. These processes are dominant in the angular region covered by our particle multi-detector. Therefore, before showing the results on the  $\gamma$ -ray spectra detected in coincidence with particles, we describe the criteria adopted to select the fragment channels.

A main point of this measurement is that the geometrical symmetry and the angular range covered by the particle detector system allow to detect, in about 10%of the collected events, multiple coincidences in which at least 2  $\gamma$ -

rays and 2 particles are detected. These events correspond mainly to the detection of the two reaction partners in kinematical coincidence.

The statistics collected for these multiple coincidence events is enough to characterize the binary processes but it is not sufficient for the study of  $\gamma$ -ray spectra properties in the GDR region.

Therefore our analysis on  $\gamma$ -ray pre-equilibrium emission is performed on the much more frequent events produced by the  $\gamma$ -1 particle coincidences. They are selected by finding a set of conditions through an iterative procedure. The charge interval, the upper thresholds on kinetic energies of the fragments are selected in such a way that the spectra of different quantities (charge distributions, c.m. angle distribution etc.) obtained from the binary coincidence events show behaviours very similar to the spectra corresponding to the  $\gamma$ -1 particle events.

The results of this procedure are the following: the charge of the selected fragments varies within the interval  $Z=14-22$ , and the laboratory kinetic energy  $T_{lab}$  is at the most 160 MeV. Under this condition we can use the  $\gamma$ -1 particle events to study the GDR properties, and the related  $\gamma$ -2 particles events to better characterize the binary break-up of the intermediate system.

In other words in this way, on average, we select a region of the phase space for which the binary coincidence events represent a restricted sample of events (due to the limited geometrical efficiency of the multi-detector) which are generated essentially by the same reaction mechanism which produces the  $\gamma$ -1 particle selected events.

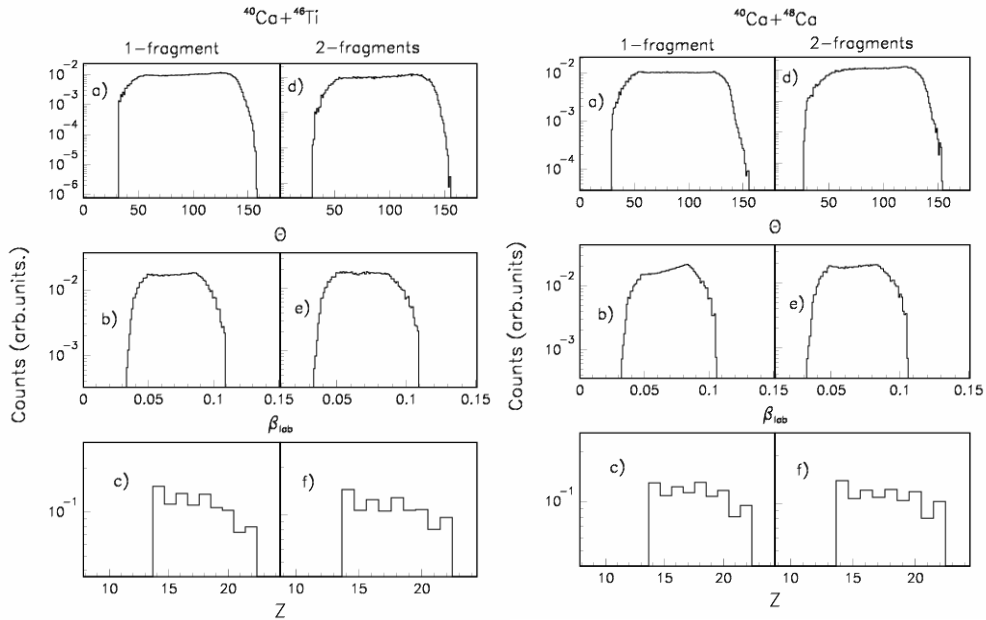


**FIGURE 4.** Different quantities as deduced from the data analysis of the investigated systems are plotted for  $\gamma$ -1-fragment and  $\gamma$ -2-fragments events. More details are given in the text (from ref.[38]).

In Figure 4. we show an example of comparison between the selected experimental  $\gamma$ -1-fragment and the  $\gamma$ -2-fragments spectra for the  $^{40}\text{Ca}+^{48}\text{Ca}$ ,  $^{40}\text{Ca}+^{46}\text{Ti}$  systems.

In particular, in the panels a) and d), we show the c.m. angular distribution of the detected fragments. In panels b) and e) we show the  $\beta_{lab}=v_{lab}/c$  spectra. Finally, in panels c) and f) we compare the charge distributions in the two cases. The quite similar behaviour of the two ensembles of spectra is evident. The comparison between the two figures shows that the selected processes for the two systems are quite similar.

We note also that in more than 90% of the selected binary events correspond to the quasi-symmetric break-up of the system with more than 70% of the total charge detected.

## $\gamma$ -ray yields

In Figure 5 (points) we show the  $\gamma$ -ray yields for the two studied systems obtained under the same selected conditions specified in the section above.

The vertical bars represent the uncertainty due to the collected statistics. The horizontal ones represent the uncertainty on the  $\gamma$ -ray energy due to the energy calibration and to the larger binning performed at higher energy to improve the counting statistics.

The black lines are statistical model calculations. The red line represents the final result which takes in to account also the contribution of the dynamical effects. Both the statistical and dynamical calculations will be discussed in the next sections. All the calculations have been convoluted with the BaF<sub>2</sub> response functions.

In the inset of the same figure we show, as a function of the  $\gamma$  energy, the ratio  $F=Y_{48\text{Ca}}^{\text{exp}}/Y_{46\text{Ti}}^{\text{exp}}$  between the yields obtained for the two systems. In the region between 12-17 MeV it is evident an extra-yield of the system  $^{40}\text{Ca}+^{48}\text{Ca}$  when compared to the  $^{40}\text{Ca}+^{46}\text{Ti}$  one.

To produce such differences, according to the statistical model, it should be necessary a 35% increase of the excitation energy (temperature effects) of the compound and of the fragments, or a variation of the produced charge distribution at a level of about 50%. This is not the case of our experimental results, as can be clearly seen by looking at Figs.3-5. In fact, the behaviours related to different quantities, deduced from the particle analysis, are quite similar for the two investigated systems.

This evidence therefore strongly suggests that we are in the presence of dynamical effects originated by the only prominent difference characterizing the two systems: the charge/mass ratios in the entrance channels.

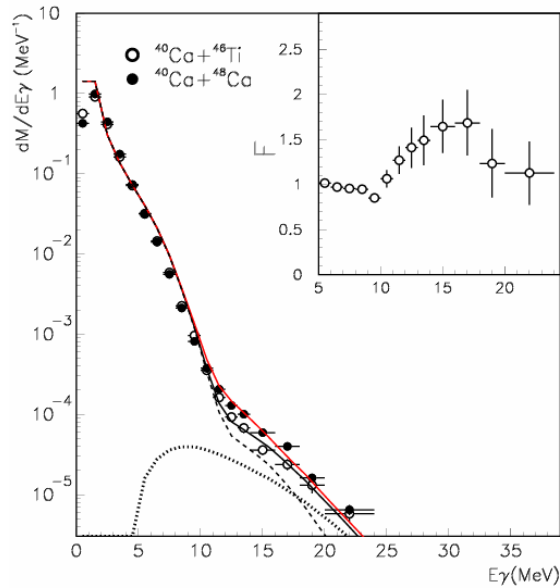


**FIGURE 5.**  $\gamma$ -ray spectra for  $^{40}\text{Ca}+^{48}\text{Ca}$  and  $^{40}\text{Ca}+^{46}\text{Ti}$  systems at 10 MeV/nucleon are shown. The lines represent calculations. In the inset the ratio between the experimental yield  $F=Y_{48\text{Ca}}^{\text{exp}}/Y_{46\text{Ti}}^{\text{exp}}$  is also displayed. More details are given in the text (from ref.[38]).

### *Dynamical interpretation of the observed extra-yield and isospin equilibration*

To describe the dynamical excitation of this pre-equilibrium mode we will use the CoMD-II model [33]. In the CoMD-II model, unlike other semi-classical microscopic models, the conservation of the total angular momentum is fulfilled.

The ensemble average of the dipolar signals generated in many replications, or events, of the same system gives the average dynamical effect. The dynamical calculations were performed using a Skyrme I effective interaction with a compressibility  $K=210$  MeV and an isospin interaction consistent with the liquid-drop mass formula [29].

The nucleon-nucleon hard-core repulsive interaction was simulated by means of free nucleon-nucleon elastic processes with a cross-section having a 50 mbarn upper limit.

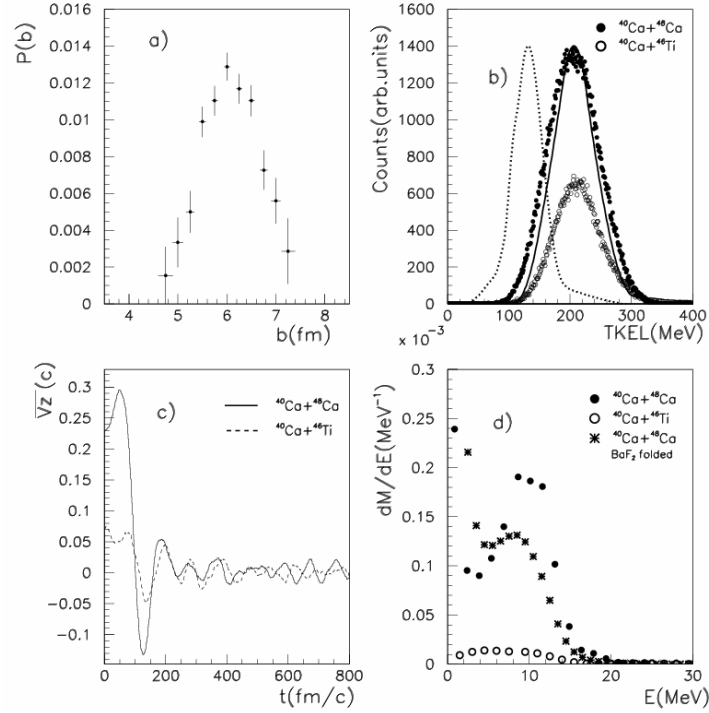


**FIGURE 6.** CoMD II results are shown with a comparison with the experimental TKEL spectrum. More details are given in the text (from ref.[38]).

The systems  $^{40}\text{Ca}+^{48}\text{Ca}$  and  $^{40}\text{Ca}+^{46}\text{Ti}$  at 10 MeV/nucleon were studied by generating several thousand of events at different impact parameters. The dynamical evolution was followed for a time interval equal of 700 fm/c. After this time, a second stage giving the final particle decay of the excited fragments was simulated using the GEMINI code [35]. To the obtained events, we have applied the main restrictions coming from the experimental set-up (angles, identification energy threshold) and from the selections applied in the experimental data analysis (see previous section). The subset of events obtained in this way can now be compared with the experimental data. In particular we will perform on these events the ensemble average of the dipolar signals and of the other useful quantities for a description of the main selected process.

As an example of this type of analysis we show in Figure 6a), for the  $^{40}\text{Ca}+^{48}\text{Ca}$  system, the impact parameter  $b$ -window selected with the above-mentioned restriction on the generated events.

In Figure 6b) we show the calculated Total Kinetic Energy Loss (TKEL) spectrum of the primary fragments (dotted line) and the one obtained including the secondary evaporation of the excited fragments and the energy loss in the thick target (continuous line). The calculated TKEL spectra were normalized to the corresponding experimental spectrum (shown with closed circles) and smoothed with a continuous function to simplify the comparison. In the same figure we show the experimental TKEL spectrum for the  $^{40}\text{Ca}+^{46}\text{Ti}$  system. The calculated TKEL spectrum is quite similar to the experimental ones.

In Figure 6c), we show, as an example, the average first time derivative  $\overline{V_z}$ , along the  $Z$ -direction, of the dipolar signals as a function of time for  $b=6$  fm (center of the  $b$ -window) for the two investigated systems.

As can be seen from the figure the complete damping of the average oscillation develops in a time interval of about 180 fm/c. In the same time interval it is also remarkable the smallness the dipolar signal for  $^{40}\text{Ca}+^{46}\text{Ti}$  as compared to the one related to the more charge/mass asymmetric  $^{40}\text{Ca}+^{48}\text{Ca}$  system. From the calculations at different impact parameters it results that the mean lifetime of the intermediate system, changes from about 400 fm/c at around  $b=6$  fm to 200 fm/c at  $b=6.75$  fm. Therefore we mainly select processes for which the GDR of the

intermediate system is out of equilibrium for at least 40% of its lifetime. For time interval shorter than this fraction, the average pre-equilibrium dipolar signal is still present. For the two studied systems in Figure 6d) we show the  $\gamma$ -ray yields related to dynamical effects for all the impact parameters contributing to the process, including the yields produced by the modes along all directions.

They have been estimated through the Fourier transform of the second time derivative of the average dipole [14,21,24,37]. We note that the maximum of the extra-yield is around 10 MeV (circles) whereas the maximum in the measured ratio F is located in the region 12-17 MeV. Some comments on this point will be given in the next section. The calculations for the  $^{40}\text{Ca}+^{46}\text{Ti}$  system produce the same scenario concerning the fragment production, however the smaller amplitude of dipolar signal produces a  $\gamma$ -ray yield which is about a factor 20 weaker at 10 MeV, as can be seen from Figure 6d). Finally, with crossed symbols, we show the results obtained for the dynamical yield  $Y_D^f$  folded with the  $\text{BaF}_2$  response function. Both the experimental studies performed on the binary coincidence events and the CoMD-II calculations, allow the description of the main features of the intermediate system break-up for the selected processes. As an example, it results from the calculations that for the  $^{40}\text{Ca}+^{48}\text{Ca}$  system and  $b=6$  fm the following average mass-charge splitting  $A_1 \sim 47, Z_1 \sim 21$  and  $A_2 \sim 37, Z_2 \sim 17$  is observed around 700 fm/c. Some units of mass and charge are emitted in the following stage described with the GEMINI code. It results that, including this small correction, the predicted average charge splitting is in substantial agreement with the experimental one.

In particular the  $R_{NZ}$  value deduced from the average primary charge/mass break-up is about 0.2. This is a rather small value if compared with the initial one  $R_{NZ}=1.81$ . Also at larger impact parameter  $b=6.75$  fm (upper half width of the selected b-window) the final value of  $R_{NZ}$  is considerably reduced down to about 0.4. This means that in the selected binary processes, after the break-up of the intermediate system, the isospin degree of freedom evaluated through the model, on average, is almost equilibrated.

The equilibration phenomenon or the loss of memory is, on the other hand, responsible for the dipolar coherent pre-equilibrium  $\gamma$ -ray emission.

### *Dynamical calculations and GDR statistical emission*

As it was shown in the previous sections, the average pre-equilibrium dipolar signal produced in the  $^{40}\text{Ca}+^{46}\text{Ti}$  system is quite weak. For this system the  $\gamma$ -ray emission is produced essentially through the statistical mechanism and it could represent the background statistical emission produced in the  $^{40}\text{Ca}+^{48}\text{Ca}$  system.

Therefore, to estimate the statistical GDR decay coming from the intermediate system in the  $^{40}\text{Ca}+^{48}\text{Ca}$  collision and to compare it with the pre-equilibrium yields related to the average dynamics, we have to study in some detail the statistical emission from the  $^{40}\text{Ca}+^{46}\text{Ti}$  system.

In particular, we have to estimate the contribution coming from the intermediate system and the one produced by the fragments.

The dynamical calculations presented in the previous section are in substantial agreement with the data coming from the two-fragment coincidence measurement (see previous section). Therefore they allow, with a good confidence level, a trace back in time of the evolution of the studied system. In particular they allow identifying and characterizing, apart from the dynamical pre-equilibrium  $\gamma$ -ray emission, the sources which contribute to the GDR statistical  $\gamma$ -yield.

It results, for example, that for the system  $^{40}\text{Ca}+^{46}\text{Ti}$  at  $b=6$  fm the intermediate system survives up to an average time of about 400 fm/c. Moreover it produces two excited fragments with an average excitation energy of about 1.3 MeV/nucleon and mass and charge partitions which are, within 10%, similar to the ones related to the  $^{40}\text{Ca}+^{48}\text{Ca}$  system. About 15% of the calculated TKEL is due to particle emission of the hot source before it breaks-up into two fragments.

Therefore we will use the CoMD-II calculations as a reference starting point, or a guide line, in trying to reproduce in the framework of the statistical model the  $\gamma$ -ray contribution produced from  $^{40}\text{Ca}+^{46}\text{Ti}$  system. The results of the statistical model calculation are shown in Figure 6 with lines, together with the experimental data. The calculations have been convoluted with the  $\text{BaF}_2$  response functions.

To estimate the contribution produced by the two fragments (dashed line in Figure 6) we used the information coming from the microscopic calculations concerning excitation energies, masses, charge and total angular momentum. The GDR damping widths have been chosen according to the study of the systematic ranging from  $A=45$  to  $A=208$  performed in ref.[15].

In that work, based on the Landau theory applied to hot rotating nuclei, a simple phenomenological function  $\Gamma(A,T,J)$  (see Eq. (4) of the above reference) describes reasonably well the experimental data collected in this range of masses. The values for these parameters have been used as input values for CASCADE calculations [32]. The final result has been obviously obtained by summing over all the contributing impact parameters according to the b-window determined from dynamical calculations.

The contribution coming from the hot intermediate stage (excitation energy about 2.3 MeV/nucleon,  $T \sim 4$  MeV) is strongly affected by the dynamics leading to the binary break-up. It is in fact quite localized in time. Moreover, the intermediate system is strongly deformed with a prolate shape. The average ratio  $d$  between the two main axes can reach large values (about 2.4 at around 200 fm/c). Both the average values and the fluctuations around this mean value change in time.

These clear non-equilibrium features motivate a different choice in the description of the statistical  $\gamma$ -ray yield coming from this stage. As shown in the first part of this contribution, the statistical yield could be evaluated by means of a fully dynamical approach in which the spectral properties of the fluctuations on the dipolar signal are analyzed. In this case, we will try to describe this contribution in a simpler phenomenological way.

The yield has been in fact described by supposing the decay of a hot deformed and rotating source (average total spin equal to about  $50\hbar$  units) modeled through a modified sum  $L(E_\gamma, J, T)$  of two Lorentian functions and thermal exponential factor coming from the level density expression [6,30,31,14].

The modification made to the  $L(E_\gamma, J, T)$  yield is the following:

$$\frac{dM}{dE_\gamma} \equiv L'(E_\gamma, J, T) = \frac{K_s \Gamma_D}{\Gamma_D + \Gamma_{cn}} L(E_\gamma, J, T) \quad (6)$$

where  $\Gamma_D$  represents the width related to the decay time  $\tau_D$  of the dynamical dipolar mode. This time determines the strength of the coherent emission in the  $^{40}\text{Ca}+^{48}\text{Ca}$  system and well approximate the finite time necessary to excite the statistical GDR mode in the same system and in the  $^{40}\text{Ca}+^{46}\text{Ti}$  one.

According to the calculation performed in the present work  $\Gamma_D$  is about 4 MeV (see Figure 7d).  $\Gamma_{cn}$  takes into account the intermediate system lifetime including the binary decay width as estimated from CoMD-II calculations. Finally  $K_s$  is a correction factor representing the emission from different steps of the cascade before the break-up. We have considered as fit parameters the  $K$  factor, the energy centroid  $E_0$  of the two Lorentian and the associated damping width  $\Gamma(0, T)$ . The results of the fit for  $^{40}\text{Ca}+^{46}\text{Ti}$  system are the following:  $K_s=3.2 \pm 0.8$ ,  $E_0=16 \pm 1.5$  MeV and  $\Gamma(0, T)=11.5 \pm 1$  MeV.

The sum of the convoluted contributions of the fragments (dash line) and the one associated to the intermediate system (dot line) are plotted in Figure 6 with a continuous black line.

From the figure it is possible to see that at 12 and 17 MeV, the fraction  $\alpha$  of the statistical GDR emission coming from the intermediate system with respect to the total contribution varies between 0.25 and 0.5.

#### *Comparison between statistical and dynamical $\gamma$ -ray emission: degree of coherence*

In the inset of Figure 5 we have shown the ratio  $F$  between the  $\gamma$  yield produced in the  $^{40}\text{Ca}+^{48}\text{Ca}$  collision respect to the  $^{40}\text{Ca}+^{46}\text{Ti}$  one. Within the errors a maximum of the average trend,  $F \sim 1.7$ , can be identified around 15 MeV. The effectiveness of the convoluted pre-equilibrium strength  $Y_D^f(E)$ , computed with the CoMD-II model (see Figure 6d) to explain the observed over-strength, can be evidenced by looking at Figure 5.

In Figure 5 in fact the red line represents the total calculated  $\gamma$ -ray yield estimated by summing the statistical contributions to the dynamical one. The global improvement in the quality of the fit with respect to the case in which only the statistical contribution is taken in to account, is clearly evident.

In ref.[38] we did also a comparison which is independent on the calculation based on the CASCADE model but which is still based on the hypothesis that the  $\gamma$ -ray statistical contribution produced from the  $^{40}\text{Ca}+^{48}\text{Ca}$  system is well approximated by the  $^{40}\text{Ca}+^{46}\text{Ti}$  one.

In particular the experimental ratio  $F$  is compared with the ratio  $F_n$  defined through the following relation:

$$F_n = \frac{Y_{46\text{Ti}}^{\text{exp}} + Y_D^f}{Y_{46\text{Ti}}^{\text{exp}}} \quad (7)$$

The obtained values of  $F_n$  well approximate the measured  $F$  between  $E_\gamma=13-16$  MeV, within the uncertainties related to our measurements.

We want to conclude this paragraph by characterizing, in a more quantitative way, the behaviour of the intermediate systems formed in the  $^{40}\text{Ca}+^{48}\text{Ca}$  collision with respect to the dipolar  $\gamma$ -ray emission in the GDR region. To this aim in the study illustrated in the previous section a degree of coherence  $\Phi_{ch}$  of the emitted radiation from the intermediate source was defined as a function of time.

In this case, we want to define a parameter having the same physical meaning but which can be more easily extracted from the experimental data. By assuming that the dynamical yield can be experimentally estimated as

$Y_D^{exp} = Y_{48Ca}^{exp} - Y_{46Ti}^{exp}$ , we can define the degree of coherence as follows:

$$\Phi_{ch}(E) \equiv \frac{Y_D^{exp}(E)}{Y_{cn} + Y_D^{exp}(E)} = \frac{F(E) - 1}{\alpha(E) + F(E) - 1} \quad ; \quad F(E) \equiv \frac{Y_{48Ca}^{exp}}{Y_{46Ti}^{exp}} \quad ; \quad \alpha(E) \equiv \frac{Y_{cn}}{Y_{46Ti}^{ex}} \quad (8)$$

These definitions are based on average  $\gamma$ -ray multiplicities at different  $\gamma$ -ray energies, rather than the corresponding released energy as in ref. [21].

The quantity  $Y_{cn}(E)$  is the  $\gamma$ -ray yield produced through a statistical mechanism from the hot compound which we suppose to be the same for the two studied systems. The evaluation of this quantity ( $\alpha$  coefficient), for non central collisions, asks for a model interpretation of the dynamics in processes leading to fragment production. However the use of performing experimental apparatus having a good reconstruction power for the emitted sources, can give strong restriction to the model interpretation. The ratio  $F$  by definition is a quantity directly measurable.

In particular  $\Phi_{ch}$  by definition is 0 if the dynamical contribution is zero, it reaches the maximum value 1 in the extreme situations in which the parameter  $\alpha$  is equal to 0.

For the investigated system, according to the performed study, we can estimate at  $E_\gamma=15$  MeV,  $\alpha \approx 0.5$ ,  $F \approx 1.7$  and therefore we obtain  $\Phi_{ch} = 0.6 \pm 0.2$  (practically the same value is obtained at 12 MeV). The system  $^{40}\text{Ca}+^{48}\text{Ca}$  studied in incomplete-fusion reactions at 25 MeV/nucleon [20,21,24] gives  $\alpha \approx 1$  with  $\Phi_{ch} = 0.3 \approx 0.03$  for  $\gamma$ -ray energies around 10 MeV. The difference on the extracted  $\Phi_{ch}$  parameters is due essentially to the fact that in the incomplete fusion processes at 25 MeV/nucleon we have the contribution of one source.

This hot source will emit down to the end of the cascade. Therefore the statistical emission in this case will have a relevant weight. On the contrary in the present case the binary selected events determine also the selection of intermediate sources (colder than the 25 MeV/nucleon case) which, after some hundreds of fm/c, decay into two fragments. During this relatively short time interval, the coherent emission plays a prominent role.

### *Pre-equilibrium $\gamma$ -ray emission and isospin equilibration*

The existence of a finite degree of coherence highlights [21] the formation of an intermediate system in which the GDR mode is not equilibrated for a time interval comparable to the mean lifetime of the hot sources.

During this time, the source is dominated by memory effects of the entrance channel. On the other hand, the observation of a considerable degree of coherence in the  $\gamma$ -ray emission can be assumed as a typical signal related to a considerable average isospin equilibration of the produced fragments.

This last point can be emphasized by looking at Figure 7. In the upper panel a) we show for two different cases, the average first time derivative  $V_z(t)$  of the total dipolar signals computed along the major axis of a di-nuclear system. These one-dimensional calculations are performed for simplicity in the harmonic approximation and neglecting the fluctuations in the charges and masses of the two fragments. However, we note that this schematic example does not allow for a strict comparison with the absolute yield produced through three-dimensional and self-consistent calculations like the CoMD-II ones. Nevertheless this example can well illustrate the sensitivity of the dynamical yield to the degree of equilibration of the charge/mass ratio which the system can attain. Both the signals have a mean lifetime of  $\tau_D=80$  fm/c and a main frequency corresponding to 10 MeV. The systems have the same initial values  $V_z(t)$  but different final values due to the different charge/mass or isospin equilibration degree.

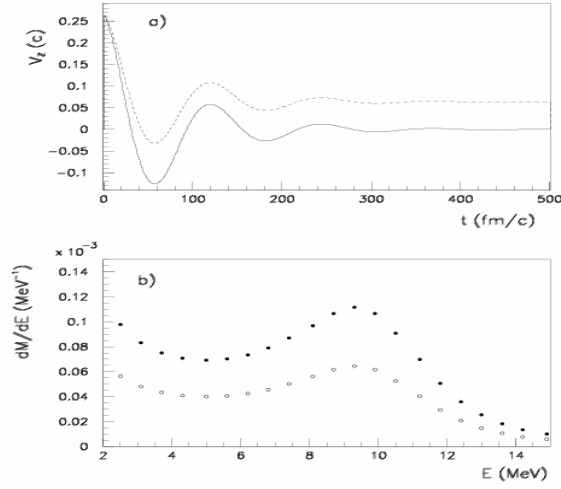


**FIGURE 7.** a) time evolution of two dipolar signals evaluated in harmonic approximation corresponding to different values of the  $R_{NZ}$  charge/mass equilibration degree. b) estimated  $\gamma$ -ray multiplicity.

Therefore we can write [28]:  $V_z(t \gg \tau_D) = R_{NZ}(t) dR/dt$ ; The last factor represents the outgoing relative velocity of the two primary fragments that in this case we suppose the same for the two systems. In such a way, a part from the degree of isospin equilibration, the two processes are strictly equivalent. In particular, the full line represents the average dipolar signal of a binary system, which has totally equilibrated the charge/mass ratios ( $R_{NZ}(t \gg \tau_D) = 0$ ), therefore  $V_z(t \gg \tau_D) = 0$ . This case can mimic the result obtained from CoMD-II calculations shown in Figure 7c for  $b = 6$  fm. In that case in fact the dipolar signal at long time is on average zero.

In the other case, displayed in Figure 10a with a dashed line, the charge/mass ratio reach about one fourth ( $R_{NZ}(t \gg \tau_D) = 0.25$ ) of the initial value. In the panel b) of the same Figure, we show the corresponding pre-equilibrium yields. The partially equilibrated system (open circles) shows a dynamical yield, and therefore a degree of coherence that is about 50% lower than the other one.

We can therefore conclude that the experimental data on  $\gamma$ -ray emission collected for the studied system together with the CoMD-II results strongly support a substantially isospin equilibration of the  $^{40}\text{Ca} + ^{48}\text{Ca}$  system obtained through the dipolar coherent emission (see Figure 7c).

Moreover the uncertainty of the experimental data on the 1-F value gives, at 14 MeV, a lower limit greater than about 0.3 (the measured value is about 0.7, see the inset in Figure 6) and therefore the schematic example discussed in this section allows estimating an upper limit for the  $R_{NZ}$  final value of about 0.5.

In a more general way we want also to note that the observation of high degree of coherence is related to the rather narrow width of the pre-equilibrium contribution generated from the average oscillations of the dipolar signal.

Moreover, the experimental evidences collected so far on this phenomenon show a degree of coherence that is clearly different from zero in a restricted region of the  $\gamma$ -ray spectrum (from 10 to 15 MeV) with values in most cases larger than 25% [9,10,11,13,14,21-24].

This means that, at the investigated incident energies (8-25 MeV/nucleon) and within the experimental uncertainties, the equilibration of the charge/mass degree of freedom could evolve through a quasi-resonant mechanism for which the damping  $\Gamma_D$  of the dynamical mode is smaller than the related resonance energy  $E_D$  ( $\pi\Gamma_D \sim E_D$ ).

This mechanism is different from the so-called ‘isospin-diffusion’ (see as examples ref [39,40]) process observed at higher energies in which, according also to the used terminology, the dipolar average collective motion should be over-damped or  $\pi\Gamma_D \gg E_D$ . In this last case we could predict a strong reduction of the extra-yield intensity (also up to one order of magnitude around 10-15 MeV) but extending in a larger  $E_\gamma$  energy interval.

This mechanism could give rise to the coherent nucleon-nucleon bremsstrahlung effect.

We now consider a generalization of Eq.(7) for realistic processes leading to many particles in the final states including the effect of fluctuations in charges, masses and momenta of the produced particles.

These conditions are typical for higher energies and we obtain the following expressions for the ensemble average of first time derivative of the total dipole  $\vec{V}$  :

$$\vec{V} = \sum_{A:Z} \frac{Z}{A} \overline{m}_{Z,A} \langle \vec{P} \rangle_{Z,A} C_{\langle p \rangle}^{Z,A}; \quad C_{\langle p \rangle}^{Z,A} = \frac{\overline{m_{Z,A} \langle \vec{P} \rangle_{Z,A}}}{\overline{m}_{Z,A} \langle \vec{P} \rangle_{Z,A}} \quad (9)$$

$$\overline{\vec{V}(t \rightarrow \infty)} = \overline{\vec{V}(t > t_{eq})} \quad (10)$$

The bar symbol indicates the ensemble average;  $\overline{m}_{Z,A}$ ,  $\langle \vec{P} \rangle_{Z,A}$  represent the average multiplicity and the mean momentum of the produced particles;  $C_{\langle p \rangle}^{Z,A}$  is the correlation function between multiplicity and the mean momentum. Therefore  $\vec{V}$  is directly linked with a kind of weighted average of the charge/mass ratio which takes into account also the average isospin flow direction via the  $\langle \vec{P} \rangle_{Z,A}$  factors. This weighted average does not depend directly on the yield of the produced free neutrons. Obviously, the indirect dependence is due to the total momentum conservation rule.

Finally Eq.(10) states that  $\vec{V}$  is invariant with respect to statistical emission processes which we can suppose to take place after a time  $t_{eq}$ . This last feature makes attractive the study of this global variable, in fact most of the study performed on the isospin subject are based on the measurements of isotopic distributions which on the contrary can be affected by secondary decay processes.

A demonstration of the above equations is given in Appendix B of ref.[38]. All the quantities appearing in Eq.(9) are in principle directly measurable through good charge and mass particle identification and the obtained value of  $\vec{V}$  can be associated to the primary stage of the process.

In real cases, a bias term, evaluated by studying the analogous charge/mass symmetric system, can be subtracted to take into account all the effects related to the incomplete event reconstruction.

We can therefore foresee that the natural evolution of the study performed on the subject treated in the present work, should include large efficiency measurements of the  $\gamma$ -pre-equilibrium emission in coincidence with fragments and particles (identified in charge and mass). The information  $\overline{\vec{V}(t = t_{eq})}$ ,  $\Phi_{ch}(E)$ ,  $Y_D^{exp}$  extracted from these measurements can give a fully understanding of the charge/mass equilibration processes that includes, its strength, the mechanism through which it evolves (quasi-resonant or over-damped motion) and the characteristic involved time. The related time scale can be in fact evaluated through the study of the spectral properties of the associated pre-equilibrium  $\gamma$ -ray emission.

Obviously, these studies are in principle related to the main ingredients of the nucleon-nucleon effective interaction, in particular the isovectorial one, allowing to obtain a useful reference point for a better knowledge of the nuclear forces.

#### IV. CONCLUSIVE REMARKS

In this contribution recent results obtained on the GDR  $\gamma$ -ray emission induced through central and mid-peripheral reaction on the  $^{40}\text{Ca}+^{48}\text{Ca}$  system, have been illustrated

The nature of this phenomenon, observed on different systems from different groups in the last 10-15 years, is well established and clearly related to the charge/mass asymmetry in the entrance channel of the studied systems. The theoretical interpretation has also attracted the attention of different theoreticians which have been able to give explanations by using different approaches.

In this contribution the interpretation of the illustrated experimental data has been performed by using the CoMD and CoMD-II semi-classical N-body approaches. The molecular dynamics approach allows having access to the average dynamics, to the fluctuating one, and to the fragment formation process. It therefore can show how the intensity of the observed pre-equilibrium  $\gamma$ -ray yield and its spectral properties gives a direct probe of other

interesting phenomena concerning the dynamics of the hot nuclear matter. One of these is the existence of a limiting excitation energy for the excitation of the dipolar mode another is linked with the isospin equilibration phenomena. To put in evidence these aspects the pre-equilibrium effect has been studied by defining a degree of coherence of the emitted radiation  $\Phi_{ch}$ , and by expressing the average time derivative  $\bar{V}$  of the dipolar signals in terms of the particle average multiplicity and momenta. The study of the behavior of these two observables allows to completely characterizing the two above mentioned aspects in an almost independent way from secondary evaporation processes.

## REFERENCES

1. J.O.Newton, B.Herskind, R.M.Diamond, E.L.Dines, J.E.Draper, H.K.Lindenberger, C.Shuck, S.Shih and S.Stefens, *Phys. Rev. Lett.* **46**, 1383 (1981).
2. K.A.Snover, *Annu. Rev. Nucl. Part. Sci.* **36**, 545 (1986).
3. M.Thoennessen, D.R.Chakrabarty, M.G.Herman, R.Butsch and P.Paul, *Phys. Rev. Lett.* **59**, 2860 (1987).
4. J.J.Gaardhoje, A.M.Bruce and B.Herskind, *Nucl. Phys. A* **482**, 121c (1988).
5. V.V.Kamanin, A.Kugler Yu, G.Sobolev and A.S.Formicheu, *Z. Phys. A* **337**, 111 (1990).
6. David Brink, *Nucl. Phys. A* **519**, 3c (1990).
7. Y.Alhassid and B.Bush, *Nucl. Phys. A* **509**, 461 (1990).
8. J.J. Gaardhoje, *Annu. Rev. Nucl. Part. Sci.* **42**, 483 (1992).
9. L.Campaiola et al., *Nucl. Phys. A* **583**, 119 (1995).
10. L.Campaiola et al., *Z. Phys. A* **352**, 421 (1995).
11. S.Flibotte et al., *Phys. Rev. Lett.* **77**, 1448 (1996) and reference therein.
12. T.Suomijarvi et al., *Phys. Rev. Lett. C* **53**, 2258 (1996).
13. F.Amorini et al., *Phys. Rev. C* **58**, 987 (1998).
14. M.Papa et al., *Eur. Phys. J. A* **4**, 69 (1999).
15. D.Kusnezov, Y.Alhassid and K.A.Snover, *Phys. Rev. Lett.* **81**, 542 (1998).
16. B.Bush and Y.Alhassid, *Nucl. Phys. A* **531**, 27 (1991).
17. K.A.Snover, *Nucl. Phys. A* **687**, 337c (2001).
18. N.P.Shaw et al., *Phys. Rev. C* **61**, 044612 (2000).
19. S.K.Hui et al., *Phys. Rev. C* **62**, 054604 (2000).
20. S.Tudisco et al., *Europhys. Lett.* **58**, 811 (2001).
21. M.Papa et al., *Phys. Rev. C* **68**, 034606 (2003).
22. D.Pierrousakou et al., *Eur. Phys. J. A* **16**, 423 (2003).
23. D.Pierrousakou et al., *Eur. Phys. J. A* **17**, 71 (2003).
24. F.Amorini et al., *Phys. Rev. C* **69**, 014608 (2004).
25. P.Heckman et al., *Nucl. Phys. A* **750**, 245 (2005).
26. J.Seitz et al., *Nucl. Phys. A* **750**, 175 (2005).
27. A.Bonasera et al., *Riv. Nuovo Cimento* **23**, 2 (2001) and reference therein.
28. See the contribution of D.Santanocito, and reference therein.
29. M.Papa, T.Maruyama and A.Bonasera, *Phys. Rev. C* **64**, 024612 (2001).
30. P.F.Bortignon et al., *Nucl. Phys. A* **583**, 101c (1995).
31. Ph.Chomaz, M.Di Toro and A.Smerzi, *Nucl. Phys. A* **563**, 509 (1993).
32. F.Puhlhofer, *Nucl. Phys. A* **280**, 267 (1977).
33. M.Papa, G.Giuliani and A.Bonasera, *J. Comp. Phys.* **208**, 403 (2005).
34. A.Musumarra et al., *Nucl. Instr. and Meth. A* **370**, 558 (1996) and reference therein.
35. A.Musumarra et al., *Nucl. Instr. and Meth. A* **409**, 414 (1998).
36. J.Lu et al., *Nucl. Instr. and Meth. A* **471**, 374 (2001).
34. G.Casini, P.R.Maurenzing, A.Olmi and A.A.Stefanini, *Nucl. Instr. and Meth. A* **277** 445 (1989).
35. J.Charity et al., *Nucl. Phys. A* **483**, 371 (1988).
36. C.Simenel, Ph.Chomaz and G. de France, *Phys. Rev. Lett.* **86**, 2971 (2001).
37. V.Baran, D.M.Brink, M.Colonna and M.Di Toro, *Phys. Rev. Lett.* **87**, 182501 (2001).
38. M.Papa et al; to be printed in *Phys. Rev. C*. and reference therein.
39. L.Shi and P.Danielewicz, *Phys. Rev. C* **68**, 064604 (2003).
40. B.A.Li, *Phys. Rev. C* **69**, 034614 (2004).